Inventory of Supplemental Items:

Figure S1, related to Figure 1: Generation of the cellular A-body

Additional characterization of the amyloid-like nature of subnuclear A-bodies. The *in situ* presence of these structures and the rIGSRNA is also demonstrated.

Figure S2, related to Figure 2: A-bodies are distinct from other subcellular structures

Detection of distinct subcellular bodies under standard literary conditions in established cell lines. The formation of non-amyloidogenic bodies is not effected by inhibition of the rIGSRNA transcripts.

Figure S3, related to Figure 3: The A-body is a heterogeneous population of proteins with similar characteristics to the total detected proteome

Bioinformatic analysis and validation of the SILAC-MS analysis performed in Figure 3.

Figure S4, related to Figure 4: Targets of the A-body possess amyloidogenic potential

Mapping of the amyloid converting motifs of VHL, cdk1, HAT1 and HDAC2.

Figure S5, related to Figure 5: APP and β-amyloid are targets of physiological amyloidogenesis

Expansion of the stress-specific and region-specific domains of amyloid precursor protein that associate with the A-bodies.

Figure S6, related to Figure 6: Physiological amyloidogenesis and disaggregation require rIGSRNA and heat shock protein activity

Controls for heat shock chaperone inhibitors used in Figure 6C. A schematic timeline is presented for drug treatment.

Figure S7, related to Figure 7: Acidosis induces cellular dormancy in an rIGS$_{28}$RNA-dependent manner

Data demonstrating the proliferative arrest associated with rIGS$_{28}$RNA-mediated A-body formation.

Table S1, related to Figure 3: SILAC-MS data for proteins targeted to acidotic A-bodies

Enrichment of proteins in the A-body of acidotic cells, relative to untreated and hypoxic fractions.

Supplementary Experimental Procedures

Supplementary References

Figure S1: Generation of the cellular A-body, related to Figure 1

(A) Specific cellular stimuli induce amyloidogenesis. VHL-GFP expressing MCF-7 cells were exposed to acidosis, heat shock, sodium arsenite, H_2O_2, thapsigargin, transcriptional stress or cycloheximide for the indicated times prior to Amylo-Glo staining (blue inset). **(B)** Amyloidophilic dyes co-localize with VHP-GFP to the A-bodies. MCF-7 cells expressing VHL-GFP were stained with Congo red (red), NIAD4 (red), Methyoxy-X04 (blue), BSB (blue) and Amylo-Glo (blue). Selected regions (white box) were expanded below with merged image included (far right panel). **(C-D)** The cellular A-bodies stains with numerous amyloid-specific dyes. **(C)** MCF-7, PC3 and **(D)** WI-38 cells were left untreated, exposed to extracellular acidosis, heat shock, transcriptional stress (actinomycin D and MG132) or allowed to recover under standard growth conditions, post-acidosis, for 24 hours. Formaldehyde-fixed cells were stained with the amyloid dyes; Congo red, Amylo-Glo, Thioflavin S, NIAD4, Methyoxy-X04 and BSB. **(E)** A-bodies can be detected in live cells. Unfixed MCF-7 cells treated, as above, were stained with Thioflavin S. **(F)** Amyloidogenesis and rIGSRNA are present *in situ*. Cryo-sectioned human brain and pancreas were stained with Congo red and B23. Congo red-positive (white arrows) and -negative (yellow arrows) A-bodies/nucleoli are indicated (left panel). RNA from human tissues were analyzed by RT-PCR for expression of the $rIGS_{16}$RNA, $rIGS_{22}$RNA and $rIGS_{28}$RNA transcripts. β-actin was used as a loading control (right panel). **(G)** Proteinase K resistant A-body fibers are composed of small fibril-like structures. MCF-7 cells, with or without proteinase K digestion, were treated for 1 hour at 43^{o}C or in acidotic media and were visualized by transmission electron microscopy. Identical 300,000x magnification images are presented (left two panels) with potential fibril-like structures indicated (yellow dashed lines). **(H)** Proteinase K unmasks the amyloid epitope within A-bodies. Heat shock treated MCF-7 cells, with or without proteinase K digestion, were stained with the OC antibody, an antibody that detects the amyloid conformation independent of the amino acid sequence. No primary antibody was used as a negative control, with images taken at the same exposure as OC antibody samples. Cytoplasmic signal is non-specific signal associated with the primary antibody. **(I)** Amyloidogenesis correlates with rIGSRNA expression. MCF-7 were exposed to acidotic media or heat shock for the indicated times. Environmental stressors were removed after three hours and cells were allowed to recover. RT-PCR quantification of the $rIGS_{28}$RNA, $rIGS_{22}$RNA and $rIGS_{16}$RNA expression levels are presented. β-actin was used as a loading control. **(J)** Knockdown efficiency of the stable shRNA cell lines. MCF-7 parental, control, $rIGS_{22}$RNA and $rIGS_{28}$RNA (two different target sites)-specific shRNA cell lines were tested for the knockdown efficiency of the $rIGS_{22}$RNA and $rIGS_{28}$RNA transcripts by RT-PCR. Actin and total RNA are loading controls. Dashed circles represent nuclei. White scale bars represents 20μm**.** White TEM scale box represent 0.1μm.

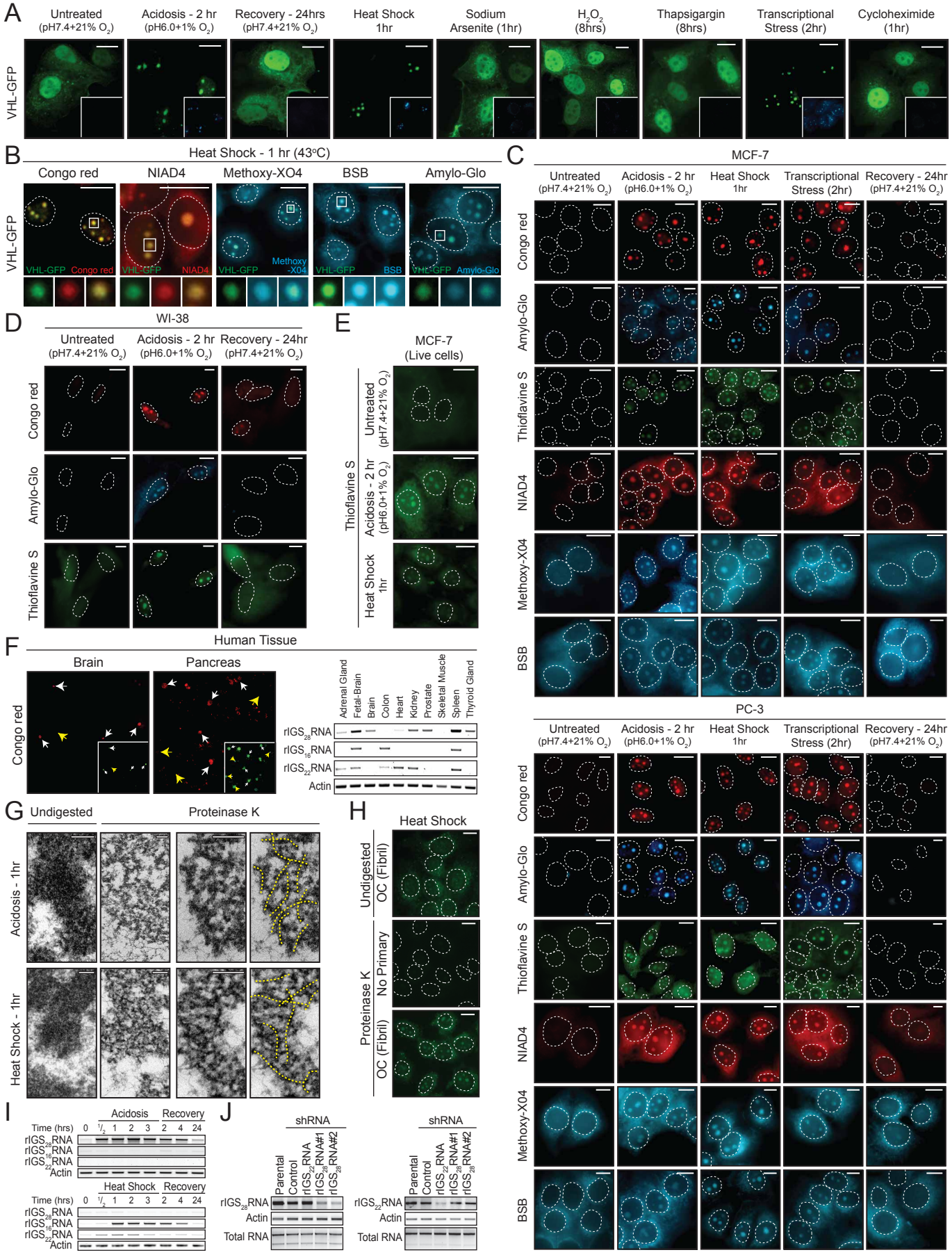
A
Untreated (pH7.4+21% O2)
Acidosis - 2 hr (pH6.0+1% O2)
Recovery - 24hrs (pH7.4+21% O2)
Heat Shock 1hr
Sodium Arsenite (1hr)
H2O2 (8hrs)
Thapsigargin (8hrs)
Transcriptional Stress (2hr)
Cycloheximide (1hr)
VHL-GFP
B
Heat Shock - 1 hr (43°C)
Congo red
NIAD4
Methoxy-XO4
BSB
Amylo-Glo
VHL-GFP
C
MCF-7
Untreated (pH7.4+21% O2)
Acidosis - 2 hr (pH6.0+1% O2)
Heat Shock 1hr
Transcriptional Stress (2hr)
Recovery - 24hr (pH7.4+21% O2)
Congo red
Amylo-Glo
Thioflavine S
NIAD4
Methoxy-X04
BSB
PC-3
D
WI-38
E
MCF-7 (Live cells)
F
Human Tissue
Brain
Pancreas
Adrenal Gland
Fetal-Brain
Brain
Colon
Heart
Kidney
Prostate
Skeletal Muscle
Spleen
Thyroid Gland
rIGS28RNA
rIGS16RNA
rIGS22RNA
Actin
G
Undigested
Proteinase K
Acidosis - 1hr
Heat Shock - 1hr
H
Heat Shock
Undigested
OC (Fibril)
Proteinase K
No Primary
I
Acidosis
Recovery
Time (hrs)
Heat Shock
J
shRNA
Parental
Control
rIGS22RNA
rIGS28RNA#1
rIGS28RNA#2
Total RNA

Figure S1

Figure S2: A-bodies are distinct from other subcellular structures, related to Figure 2

(A-C) Other cellular structures do not stain with the amyloidophilic dye Congo red. MCF-7 (A) and PC-3 (B-C) cells were grown under the indicated conditions prior to fixation and detection of subcellular bodies with the noted antibody (green). All cells were co-stained with Congo red and overlaid images are presented, with magnified regions (white box) expanded below and presented as the green (left) red (middle) and merge channels. Grossly over-exposed Congo red staining is included (C) to highlight the lack of amyloidogenic dye binding to the aggresome. **(D)** Knockdown efficiency of siRNA targeting established lncRNA. PC-3 cells transfected with control or siRNA targeting rIGS$_{22}$RNA, rIGS$_{28}$RNA, NEAT1, MALAT1, HOTAIR and GAPDH mRNA were exposed to heat shock or 5μM MG132 conditions. The indicated transcripts were detected by RT-PCR. Actin and total RNA are loading controls. (E) Inhibition of rIGS$_{22}$RNA and rIGS$_{28}$RNA does not impair the formation of other cellular bodies. MCF-7 cells stably expressing shRNA against rIGS$_{22}$RNA (left panels) and rIGS$_{28}$RNA (right panels) were treated as indicated and stained for subcellular body specific markers (green) and Congo red (red). Dashed circles represent nuclei. Selected regions (white box) were expanded below. White scale bars represents 20μm.

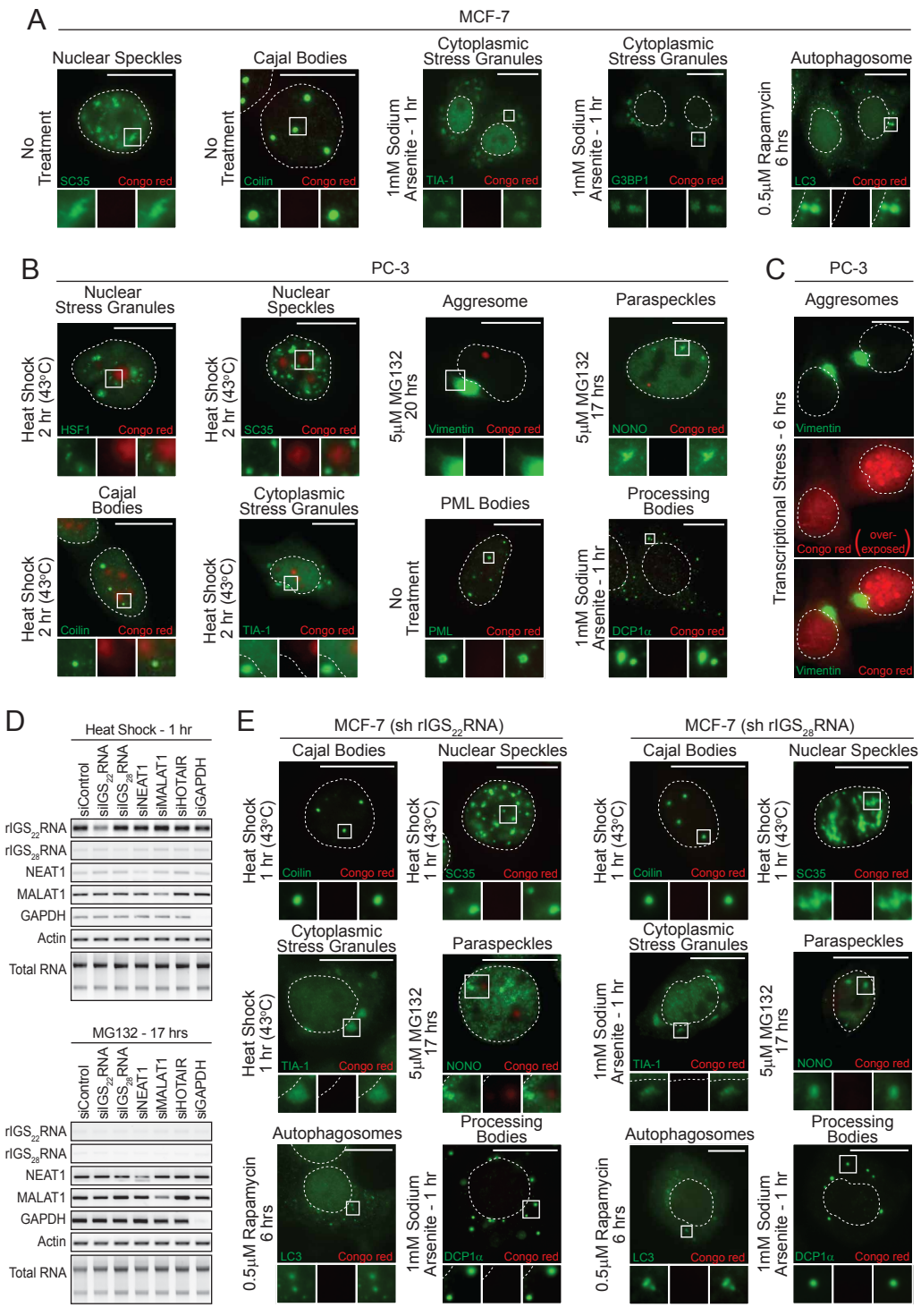
A
MCF-7
Nuclear Speckles
Cajal Bodies
Cytoplasmic Stress Granules
Cytoplasmic Stress Granules
Autophagosome
No Treatment
No Treatment
1mM Sodium Arsenite - 1 hr
1mM Sodium Arsenite - 1 hr
0.5μM Rapamycin 6 hrs
SC35
Coilin
TIA-1
G3BP1
LC3
Congo red
B
PC-3
Nuclear Stress Granules
Nuclear Speckles
Aggresome
Paraspeckles
Heat Shock 2 hr (43°C)
Heat Shock 2 hr (43°C)
5μM MG132 20 hrs
5μM MG132 17 hrs
HSF1
SC35
Vimentin
NONO
Cajal Bodies
Cytoplasmic Stress Granules
PML Bodies
Processing Bodies
Heat Shock 2 hr (43°C)
Heat Shock 2 hr (43°C)
No Treatment
1mM Sodium Arsenite - 1 hr
Coilin
TIA-1
PML
DCP1α
C
PC-3
Aggresomes
Transcriptional Stress - 6 hrs
Vimentin
Congo red
over-exposed
Vimentin
D
Heat Shock - 1 hr
siControl
siIGS22RNA
siIGS28RNA
siNEAT1
siMALAT1
siHOTAIR
siGAPDH
rIGS22RNA
rIGS28RNA
NEAT1
MALAT1
GAPDH
Actin
Total RNA
MG132 - 17 hrs
E
MCF-7 (sh rIGS22RNA)
MCF-7 (sh rIGS28RNA)
Cajal Bodies
Nuclear Speckles
Cytoplasmic Stress Granules
Paraspeckles
Autophagosomes
Processing Bodies
Heat Shock 1 hr (43°C)
5μM MG132 17 hrs
0.5μM Rapamycin 6 hrs
1mM Sodium Arsenite - 1 hr
Coilin
SC35
TIA-1
NONO
LC3
DCP1α
Congo red

Figure S2

Figure S3: The A-body is a heterogeneous population of proteins with similar characteristics to the total detected proteome, related to Figure 3

(A) A heterogeneous family of proteins are targeted to the cellular A-bodies. Distribution of protein size (kDa) (left panel), isoelectric point (pI) (middle panel) and grand average of hydrophobicity (GRAVY) scores (right panel) for the total (838 proteins) and A-body-specific (184 proteins) populations. Isoelectric point and GRAVY scores were calculated using the ProtParam program (SIB ExPASy Bioinformatics Resource Portal). The GRAVY score for each protein was calculated as the sum of hydropathy values of all the amino acids, divided by the number of residues in the protein. **(B)** Validation of SILAC-MS candidate proteins. Normoxic/neutral, hypoxic/neutral and hypoxic/acidotic treated MCF-7 cells were harvested and whole cell lysates (WCL), cytoplasmic (Cyto), nuclear (Nuc) and nucleolus/A-body fractions were analyzed by western blot with antibodies against the catalytic subunit of DNA polymerase delta (POLD1), spliceosome RNA helicase (UAP56), 14-3-3ζ, elongation factor 1β (eEF1B2), transcription initiation factor 1β (TIF-1β), histone acetyltransferase-1 (HAT-1) and cyclin-dependent kinase 1 (cdk1). Nucleolar transcription factor-1 (UBF1) and cyclin G were used as loading controls. **(C-D)** SILAC-MS candidates co-localize with the amyloid dye Amylo-Glo. PC-3 (C) and MCF-7 (D) cells were grown under hypoxic/acidotic conditions and analyzed by indirect immunofluorescence microscopy for endogenous HAT1, TIF-1β, cdk1 and PCNA. Amylo-Glo images of the same field were captured (blue). **(E)** SILAC-MS candidates are targeted to nuclear foci. PC3 cells were grown in normoxia/neutral, hypoxia/neutral and hypoxia/acidosis conditions and analyzed by indirect immunofluorescence microscopy for endogenous UAP56, HAT1, TIF-1β, ATP-dependent helicase (ATRX), DNA polymerase alpha catalytic subunit (POLA1), POLD1, cdk1, replication factor C subunit 1 (RFC1), UBF1 and PCNA. **(F)** Localization of SILAC-MS candidates to subnuclear foci is dependent on rIGSRNA. MCF-7 cells stably-expressing shRNA against $rIGS_{28}$RNA (sh28#1) or a control sequence were treated and stained for endogenous proteins as in (E)**.** B23 (green) inset. Dashed circles represent nuclei. White scale bars, 20μm**.**

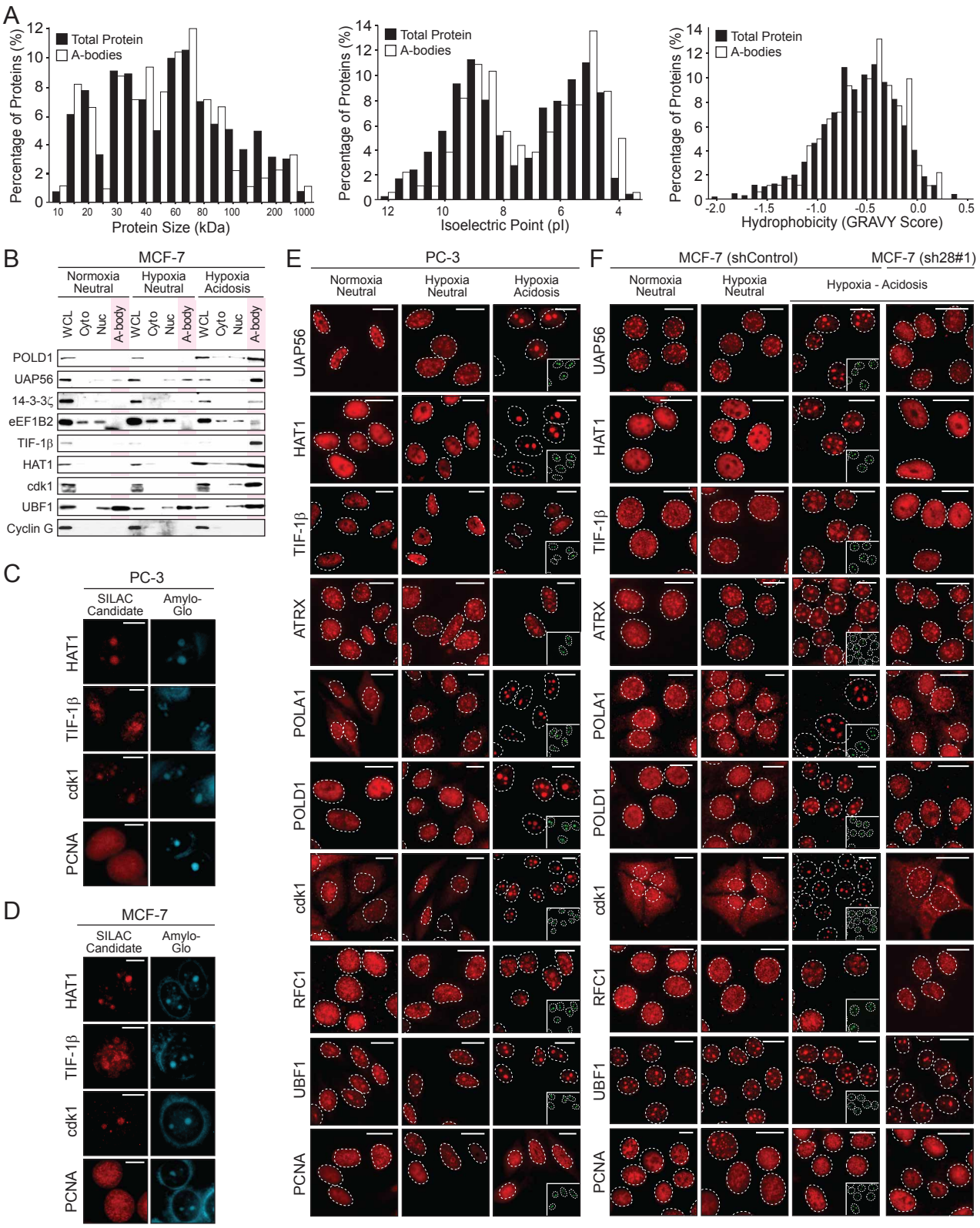
A
Total Protein
A-bodies
Percentage of Proteins (%)
Protein Size (kDa)
Isoelectric Point (pI)
Hydrophobicity (GRAVY Score)
B
MCF-7
Normoxia Neutral
Hypoxia Neutral
Hypoxia Acidosis
WCL
Cyto
Nuc
A-body
POLD1
UAP56
14-3-3ζ
eEF1B2
TIF-1β
HAT1
cdk1
UBF1
Cyclin G
C
PC-3
SILAC Candidate
Amylo-Glo
HAT1
TIF-1β
cdk1
PCNA
D
MCF-7
SILAC Candidate
Amylo-Glo
HAT1
TIF-1β
cdk1
PCNA
E
PC-3
Normoxia Neutral
Hypoxia Neutral
Hypoxia Acidosis
UAP56
HAT1
TIF-1β
ATRX
POLA1
POLD1
cdk1
RFC1
UBF1
PCNA
F
MCF-7 (shControl)
MCF-7 (sh28#1)
Normoxia Neutral
Hypoxia Neutral
Hypoxia - Acidosis
UAP56
HAT1
TIF-1β
ATRX
POLA1
POLD1
cdk1
RFC1
UBF1
PCNA

Figure S3

Figure S4: Targets of the A-body possess amyloidogenic potential, related to Figure 4

(A) UAP56, RNF8 and cdk1 target to nuclear foci and can obtain an amyloid-like conformation upon bacterial expression. UAP56-GFP, RNF8-GFP, cdk1-GFP, Ran-GFP, cdk4-GFP or the nucleolar resident protein B23-GFP were expressed in MCF-7 cells left untreated or exposed to acidosis or BL21 cells prior to staining with Congo red and Hoechst. **(B)** The central region targets VHL to the A-body. 36 amino acid fragments of VHL were fused to GFP and expressed in MCF-7 cells untreated or exposed to acidosis. Subcellular distribution of the VHL fragments was detected by fluorescence microscopy **(C)** An RH cluster and amyloidogenic region is necessary for stress-specific insolubilization. The indicated fragments of VHL or the artificial ACM (aACM) of VHL and POLD1 were fused to GFP and expressed in MCF-7 cells exposed to acidosis for 2 hours. Whole cell lysates (WCL) and insoluble fractions were harvested. Exogenous proteins were detected by western blot (GFP). GAPDH and Histone H3 were used as loading controls. **(D)** Tethering ACM or aACM sequences to GFP immobilize the fusion protein in the A-bodies. Quantification of recovery after photobleaching kinetics for the constructs listed as the mean relative intensity of at least 5 data sets. **(E)** Cdk1, HAT1 and HDAC2 contains fibril-forming peptidic regions. Results of the Rosetta-design program ZipperDB analysis of full length cdk1 and fragments of cdk1, HAT1 and HDAC2 containing an R/H cluster in close proximity to regions with fibrillation propensity. The Rosetta energy threshold of -23 kcal/mol was used as an indicator of fibril-positive regions. Fragments fused to GFP are indicated with amino acid sequence bracketed. **(F)** Mapping the ACM of VHL and cdk1. VHL (amino acids: 104-140 and 122-140) or cdk1 (amino acids: 100-130 and 100-119)-GFP were expressed in BL21 cells (stained with Congo red and Hoechst) or MCF-7 cells (stained with Hoechst) left untreated or exposed to acidosis. **(G)** An R/H cluster is essential for mammalian amyloidogenesis. HAT1 and HDAC2 fragments described above (E) were expressed in MCF-7 cells exposed to extracellular acidosis. **(H)** aACMs are sufficient to induce amyloidogenesis. aACM described above were expressed in MCF-7 cells left untreated, exposed to acidosis prior to fluorescence microscopy. Hoechst is inset. BL21 cells expressing aACM-GFP were stained with Congo red and Hoechst. X-ray diffraction was performed on BL21 inclusion bodies. Dashed circles represent nuclei (MCF-7) or whole cell (BL21). White scale bars, 20μm**.**

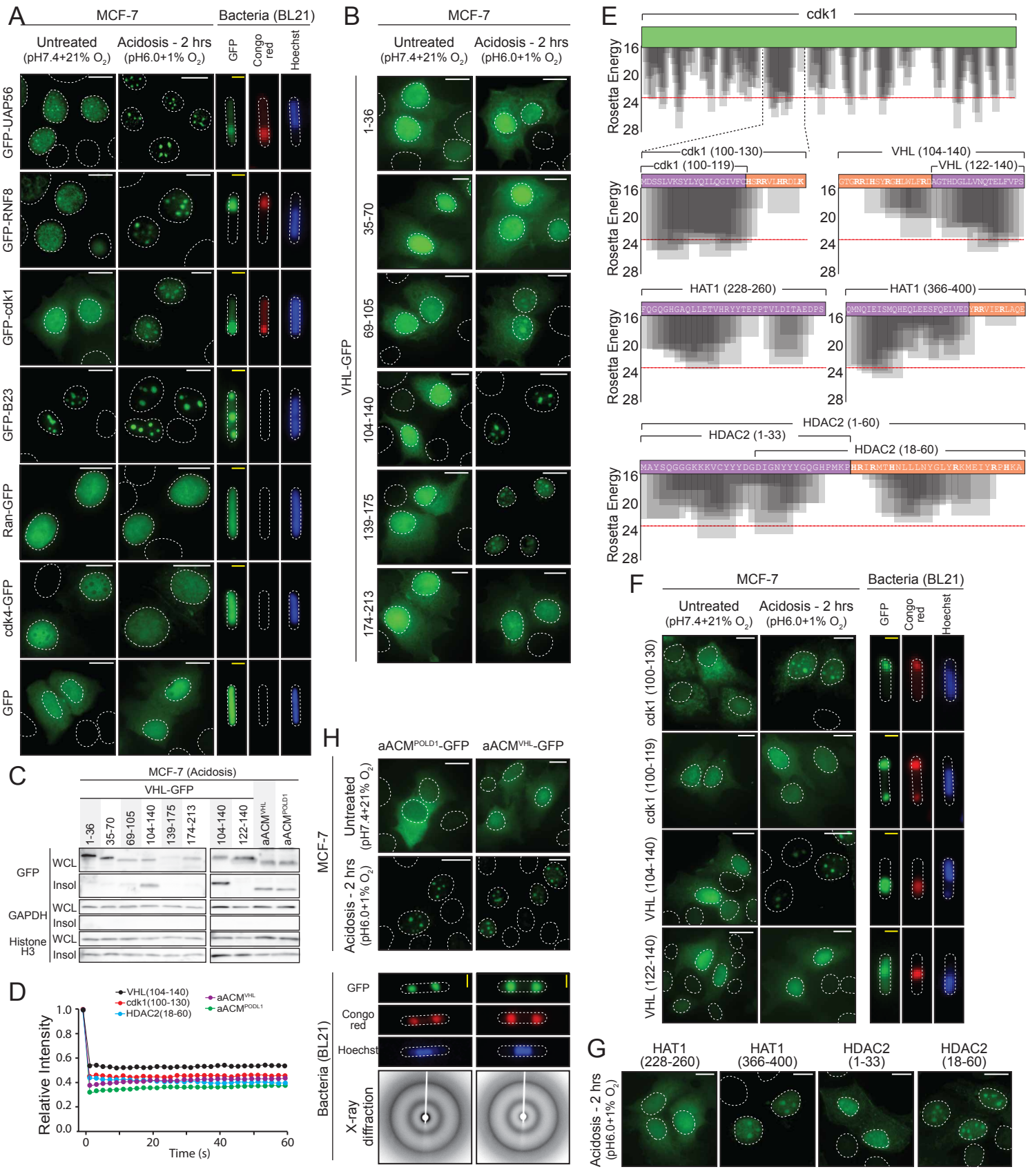
A
MCF-7
Bacteria (BL21)
Untreated (pH7.4+21% O2)
Acidosis - 2 hrs (pH6.0+1% O2)
GFP
Congo red
Hoechst
GFP-UAP56
GFP-RNF8
GFP-cdk1
GFP-B23
Ran-GFP
cdk4-GFP
GFP
B
MCF-7
Untreated (pH7.4+21% O2)
Acidosis - 2 hrs (pH6.0+1% O2)
VHL-GFP
1-36
35-70
69-105
104-140
139-175
174-213
C
MCF-7 (Acidosis)
VHL-GFP
1-36
35-70
69-105
104-140
139-175
174-213
104-140
122-140
aACMVHL
aACMPOLD1
GFP
GAPDH
Histone H3
WCL
Insol
D
VHL(104-140)
cdk1(100-130)
HDAC2(18-60)
aACMVHL
aACMPODL1
Relative Intensity
Time (s)
E
cdk1
Rosetta Energy
cdk1 (100-130)
cdk1 (100-119)
VHL (104-140)
VHL (122-140)
HAT1 (228-260)
HAT1 (366-400)
HDAC2 (1-60)
HDAC2 (1-33)
HDAC2 (18-60)
F
MCF-7
Bacteria (BL21)
Untreated (pH7.4+21% O2)
Acidosis - 2 hrs (pH6.0+1% O2)
GFP
Congo red
Hoechst
cdk1 (100-130)
cdk1 (100-119)
VHL (104-140)
VHL (122-140)
G
HAT1 (228-260)
HAT1 (366-400)
HDAC2 (1-33)
HDAC2 (18-60)
Acidosis - 2 hrs (pH6.0+1% O2)
H
aACMPOLD1-GFP
aACMVHL-GFP
MCF-7
Untreated (pH7.4+21% O2)
Acidosis - 2 hrs (pH6.0+1% O2)
Bacteria (BL21)
GFP
Congo red
Hoechst
X-ray diffraction

Figure S4

Figure S5: APP and β-amyloid are targets of physiological amyloidogenesis, related to Figure 5

(A) Schematic diagram of amyloid precursor protein (APP). Signal peptide and transmembrane domain are highlighted in yellow. α–, β–, and γ–secretase cleavage sites are indicated. The location of various truncations used are presented. **(B)** β-amyloid is targeted to subnuclear foci during specific environmental stress. The pathological β-amyloid (1-40) and non-pathological P3 (18-40) peptides were fused to GFP and expressed in MCF-7 cells left untreated or exposed to acidosis, heat shock, thapsigargin, sodium arsenite, transcriptional stress (actinomycin D and MG132) or H_2O_2 for the indicated times. **(C)** Random 42 amino acid regions of APP are not targeted to A-bodies. The indicated regions of APP or 42 amino acid fragments of this proteins were fused to GFP and expressed in untreated or acidotic MCF-7 cells. Dashed circles represent nuclei. White scale bars, 20μm**.**

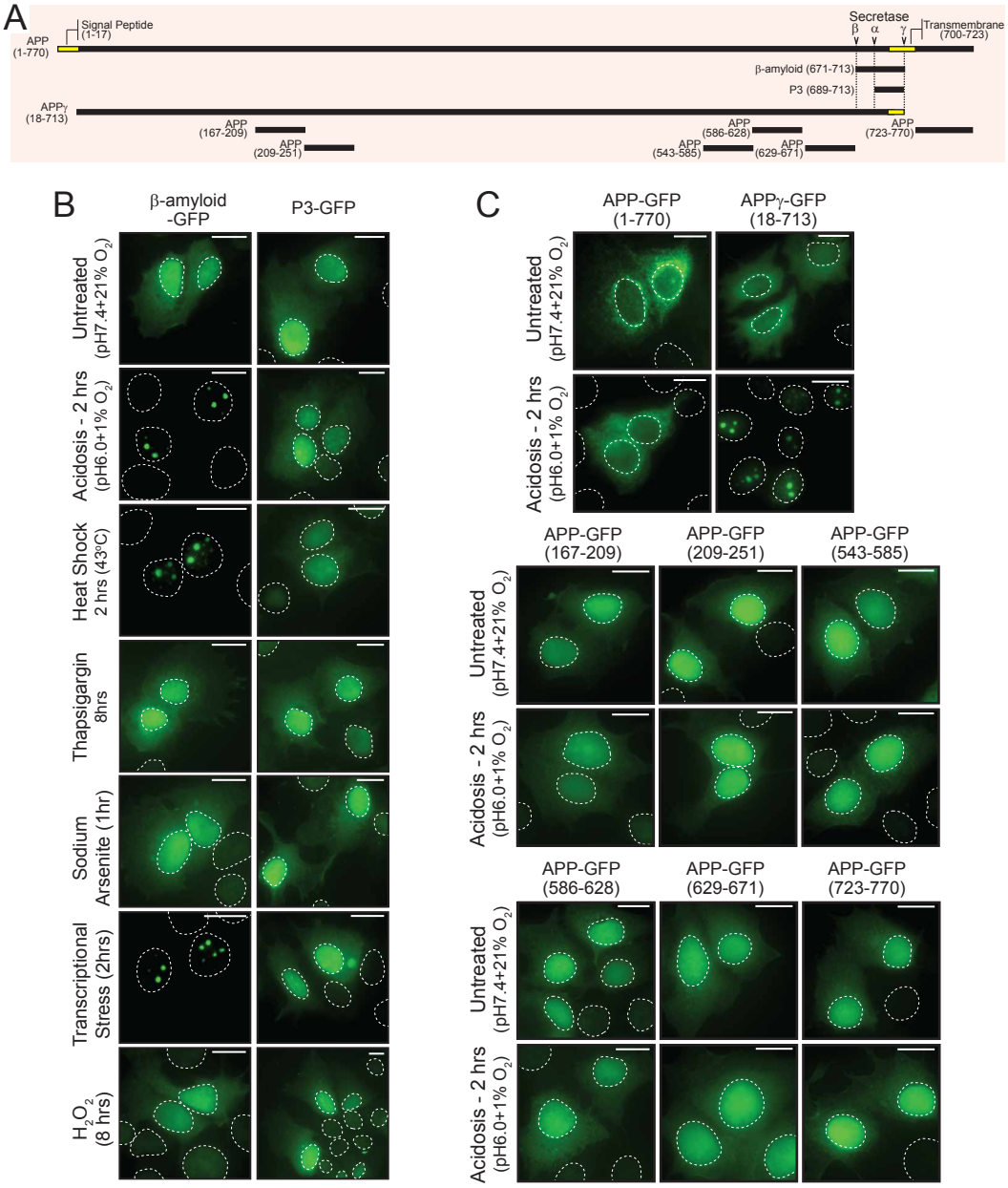
A
Signal Peptide
(1-17)
APP
(1-770)
Secretase
β α γ
Transmembrane
(700-723)
β-amyloid (671-713)
P3 (689-713)
APPγ
(18-713)
APP
(167-209)
APP
(209-251)
APP
(543-585)
APP
(586-628)
APP
(629-671)
APP
(723-770)
B
β-amyloid
-GFP
P3-GFP
Untreated
(pH7.4+21% O2)
Acidosis - 2 hrs
(pH6.0+1% O2)
Heat Shock
2 hrs (43°C)
Thapsigargin
8hrs
Sodium
Arsenite (1hr)
Transcriptional
Stress (2hrs)
H2O2
(8 hrs)
C
APP-GFP
(1-770)
APPγ-GFP
(18-713)
APP-GFP
(167-209)
APP-GFP
(209-251)
APP-GFP
(543-585)
APP-GFP
(586-628)
APP-GFP
(629-671)
APP-GFP
(723-770)

Figure S5

Figure S6: Physiological amyloidogenesis and disaggregation require rIGSRNA and heat shock protein activity, related to Figure 6

(A) Amyloid disintegration is caused by protein disaggregation, not degradation. VHL-GFP expressing MCF-7 cells were left untreated, exposed to acidosis or recovered for 4 hours with no drugs, the Hsp70 inhibitor VER155008 (VER) or the protein synthesis inhibitor cycloheximide. **(B)** Heat shock proteins are present in A-bodies as cells recover from extracellular acidosis and thermal stress. MCF-7 cells recovering from acidosis or heat shock (2 hours) were stained for Hsp27, Hsp40, Hsp60, Hsp70, Hsp90, Hsp105, HSF1, GRP78, GRP94, Calnexin, Calreticulin, and Protein Disulfide Isomerase. Congo red is inset **(C)** Schematic diagram indicating the stressing, recovery and drug treatment of MCF-7 cells exposed to chaperone inhibitors in figure 5 (C-E). **(E)** Chaperone inhibitors do not effect viability during recovery. MCF-7 cells exposed to heat shock for 3 hours were allowed to recover in media containing no drugs or the chaperone inhibitors 16F16 (5μM), EGCG (5μM), VER155008 (40μM), 17-AAG (5μM) or VER155008+17-AAG, the autophagy inhibitor wortmanin (5μM) or the protein synthesis inhibitor cycloheximide (25μg/ml) for 4 hours. Viability was detected by fluorescein diacetate (FDA) fluorescence intensity. **(E)** Chaperone inhibitor treatment does not induce physiological amyloidogenesis. MCF-7 cells expressing VHL-GFP were left untreated or exposed to the chaperone inhibitors 16F16 (5μM), EGCG (5μM), VER155008 (40μM), 17-AAG (5μM) or VER155008+17-AAG for 4 hours and stained with Hoechst (inset left) and Congo red (inset right). White scale bars, 20μm**.**

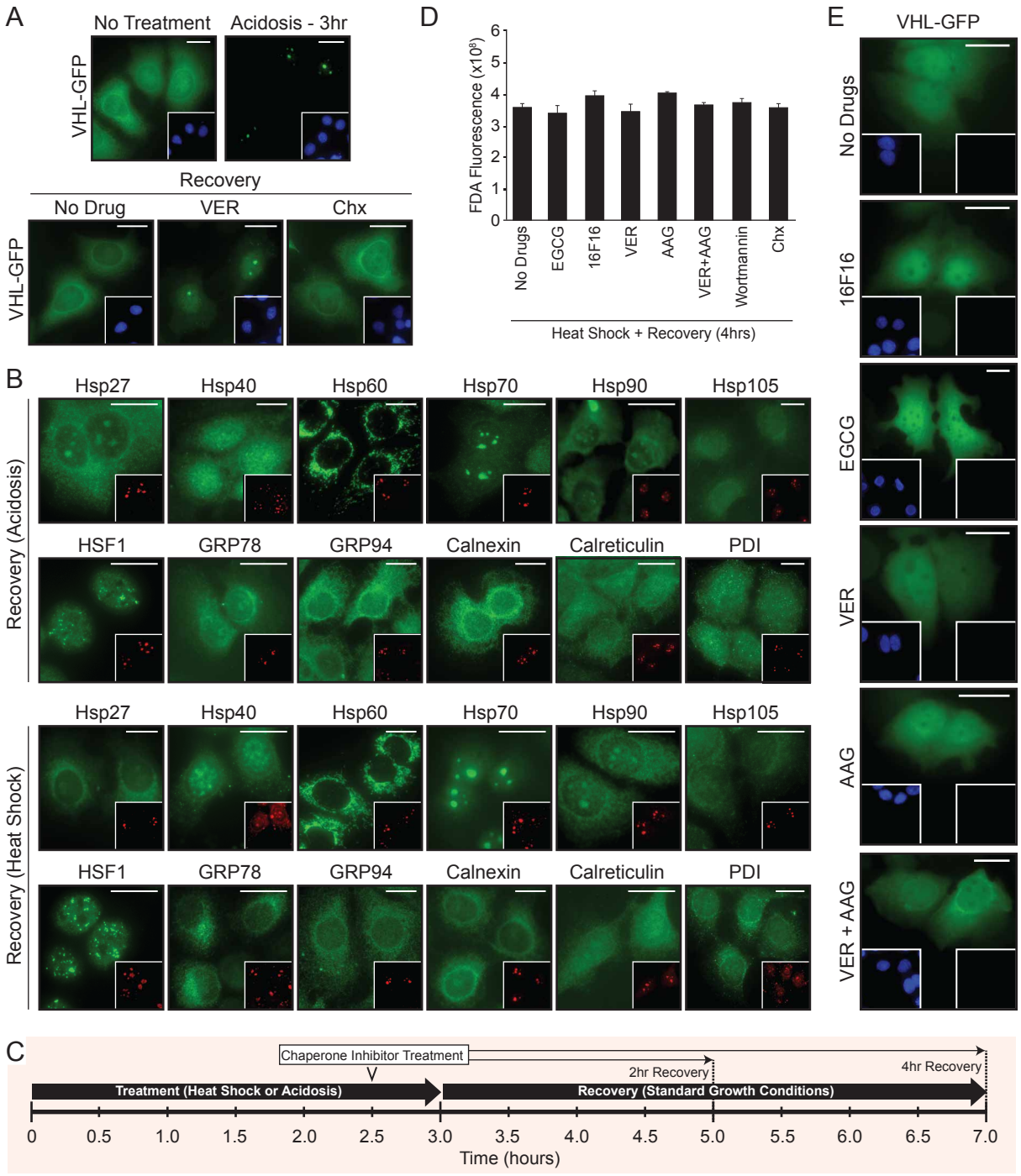
A
No Treatment
Acidosis - 3hr
VHL-GFP
Recovery
No Drug
VER
Chx
VHL-GFP
D
FDA Fluorescence (x10⁸)
No Drugs
EGCG
16F16
VER
AAG
VER+AAG
Wortmannin
Chx
Heat Shock + Recovery (4hrs)
E
VHL-GFP
No Drugs
16F16
EGCG
VER
AAG
VER + AAG
B
Hsp27
Hsp40
Hsp60
Hsp70
Hsp90
Hsp105
HSF1
GRP78
GRP94
Calnexin
Calreticulin
PDI
Recovery (Acidosis)
Recovery (Heat Shock)
C
Chaperone Inhibitor Treatment
2hr Recovery
4hr Recovery
Treatment (Heat Shock or Acidosis)
Recovery (Standard Growth Conditions)
Time (hours)

Figure S6

Figure S7: Acidosis induces cellular dormancy in an rIGS$_{28}$RNA-dependent manner, related to Figure 7

(A) Hypoxia has minimal effect on cell proliferation. MCF-7, PC-3 and WI-38 cells were incubated under standard growth conditions (21% O_2 + pH 7.4) for two days, prior to being transferred to a hypoxic environment (1% O_2 + pH 7.4). 750,000 (MCF-7 and PC-3 – left axis) or 75,000 (WI-38 – right axis) cells were initially cultured and counted daily with Trypan Blue staining to ensure viability. **(B)** MCF-7 with impaired rIGS$_{28}$RNA expression proliferate during hypoxia. MCF-7 cells stably-expressing two independent shRNA against rIGS$_{28}$RNA (sh28#1 and sh28#2) or a control sequence (shCtrl) were grown under the indicated conditions and counted as above. **(C)** Knockdown efficiency of the stable PC-3 shRNA cell lines. PC-3 parental, control and rIGS$_{28}$RNA (two clonal lines)-specific shRNA cell lines were tested for the knockdown efficiency of the rIGS$_{28}$RNA transcripts by RT-PCR. Actin and total RNA are loading controls. **(D-E)** Inhibition of rIGS$_{28}$RNA restores proliferative capacity to acidotic PC-3 cells. PC-3 lines described above (C) were exposed to hypoxia in acidosis-permissive media for the indicated times. **(D)** Live cells were counted as described above or **(E)** BrdU was added 1 hour prior to fixation and BrdU detection. Percent BrdU incorporation was calculated as BrdU-positive nuclei divided by Hoechst-positive nuclei. **(F)** Intracellular ATP levels are maintained during extracellular acidosis by rIGS$_{28}$RNA. MCF-7 cells stably-expressing two independent shRNA against rIGS$_{28}$RNA or a control sequence (shCtrl) were exposed to normoxic-neutral, hypoxic-neutral and hypoxic-acidosis conditions for 24 hours prior to assessment of intracellular ATP levels using the CellTiter-Glo Luminescent Assay. **(G)** Acidosis induces a state of cellular dormancy. MCF-7 cells stably-expressing control (shCtrl) or rIGS$_{28}$RNA (sh28#1)-specific shRNA were grown under the indicated conditions for 24 hours, prior to the addition of nocodazole (24 hours) to induce a G_2/M phase arrest in proliferating cells. Flow cytometry analysis of propidium iodide stained cells was used to assess cell cycle stage. **(H)** Inhibition of rIGS$_{28}$RNA enhances PC-3 tumor growth. Nude mouse xenograft assays with PC-3 cells expressing no shRNA, shRNA against a control sequence or shRNA targeting rIGS$_{28}$RNA (n=4). Tumor volumes were determined at two weeks post-injection (left). Endogenous HAT1 was detected by indirect immunofluorescence microscopy (B23- inset green) and hematoxylin/eosin staining was performed on paraffin-embedded sections. **(I)** Inhibition of rIGS$_{28}$RNA impairs amyloidogenesis in mouse xenografts. Paraffin-embedded MCF-7 shControl or shrIGS$_{28}$RNA xenograft sections were stained with Congo red and fluorescent *in situ* hybridization was performed to detect rIGS$_{28}$RNA. B23 (green) is inset. Results are presented as means and SEM (n=3). Significance values were calculated by a two-tailed Student's t-test; *p shown < 0.01.

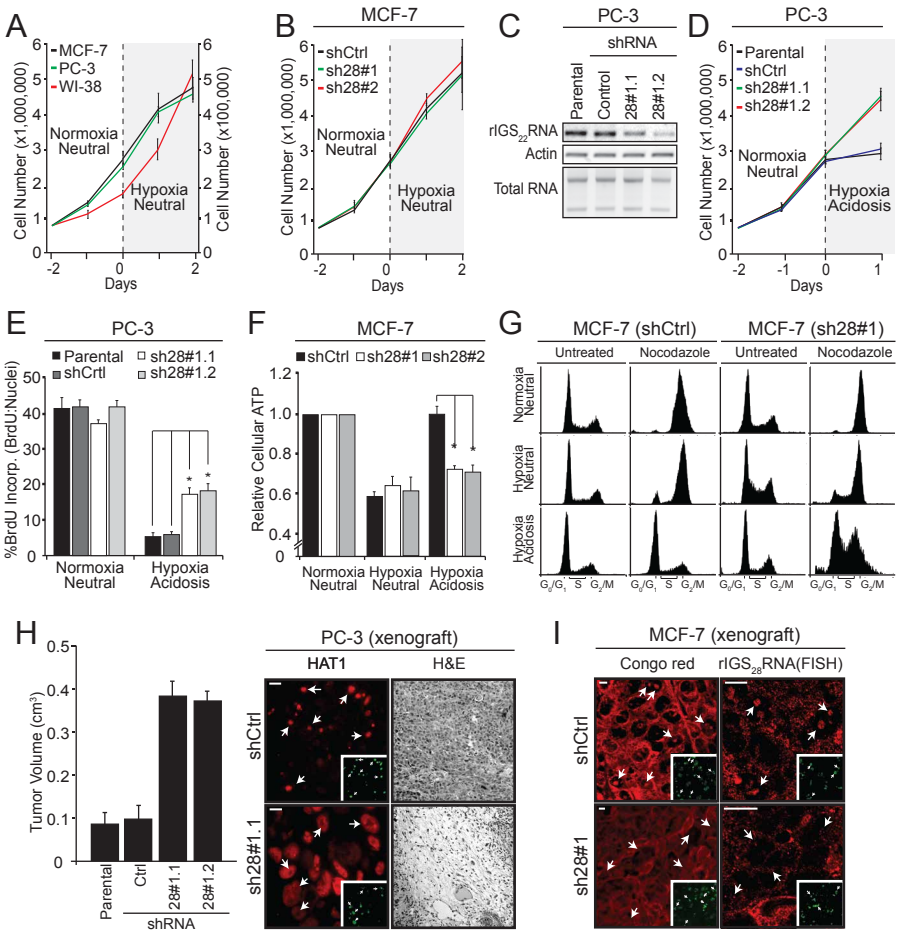
A
MCF-7
PC-3
WI-38
Normoxia Neutral
Hypoxia Neutral
Cell Number (x1,000,000)
Cell Number (x100,000)
Days
B
MCF-7
shCtrl
sh28#1
sh28#2
Normoxia Neutral
Hypoxia Neutral
Cell Number (x1,000,000)
Days
C
PC-3
shRNA
Parental
Control
28#1.1
28#1.2
rIGS22RNA
Actin
Total RNA
D
PC-3
Parental
shCtrl
sh28#1.1
sh28#1.2
Normoxia Neutral
Hypoxia Acidosis
Cell Number (x1,000,000)
Days
E
PC-3
Parental
shCrtl
sh28#1.1
sh28#1.2
%BrdU Incorp. (BrdU:Nuclei)
Normoxia Neutral
Hypoxia Acidosis
F
MCF-7
shCtrl
sh28#1
sh28#2
Relative Cellular ATP
Normoxia Neutral
Hypoxia Neutral
Hypoxia Acidosis
G
MCF-7 (shCtrl)
MCF-7 (sh28#1)
Untreated
Nocodazole
Normoxia Neutral
Hypoxia Neutral
Hypoxia Acidosis
G0/G1 S G2/M
H
Tumor Volume (cm3)
Parental
Ctrl
28#1.1
28#1.2
shRNA
PC-3 (xenograft)
HAT1
H&E
shCtrl
sh28#1.1
I
MCF-7 (xenograft)
Congo red
rIGS28RNA(FISH)
shCtrl
sh28#1

Figure S7

Table S1: SILAC-MS data comparing the relative enrichment of proteins in the A-body fractions purified from normoxia/neutral, hypoxic/neutral and hypoxia/acidotic, related to Figure 3

SILAC-MS analysis of purified (see experimental procedures) A-bodies from MCF-7 cells grown under normoxia/neutral (NN), hypoxic/neutral (HN) and hypoxia/acidotic (HA) conditions. Ratio of the relative abundance and log2 relative abundance are presented. Positive candidates possessed a <0.5 log2 relative abundance in both HN/HA and NN/HA fractions. Peaks Studio 7.0 (Thermo Scientific) software was used for protein identification and quantification.

Supplemental Experimental Procedures

Antibodies and dyes. Antibodies purchased were validated for western blotting and immunohistochemistry by the supplier. Monoclonal antibodies were used to detect 14-3-3ζ (QED Biosciences Inc.), B23 (Santa Cruz Biotechnology, sc-47725), eEF1B2 (Abnova, H00001933-M10), cdk1 (Boehringer Mannheim), Hsp27 (Cell Signaling Technology, 2402S), Hsp40 (Cell Signaling Technology, 4871), Hsp60 (Cell Signaling Technology 1216S), Hsp90 (Cell Signaling Technology, 4877), VHL (Oncogene Science, OP102), BiP/GRP78 (Cell Signaling Technology, 3177), Calnexin (Cell Signaling Technology, 2679), PDI (Cell Signaling Technology, 3501), PCNA (Santa Cruz Biotechnology, sc-25280), UBF1 (Santa Cruz Biotechnology, sc-13125), Vimentin (Santa Cruz Biotechnology, sc-6260), SC35 (Abcam, ab11826) and p54nrb/NonO (EMD Millipore, 05-950), and polyclonal antibodies detected POLD1 (Santa Cruz Biotechnology, sc-8797), POLA1 (Santa Cruz Biotechnology, sc-48818), ATRX (Santa Cruz Biotechnology, sc-15408), RFC1 (Santa Cruz Biotechnology, sc-20993), Hsp70 (Cell Signaling Technology, 4872), Hsp105 (Santa Cruz Biotechnology, sc-6241), HSF1 (Cell Signaling Technology, 4356), GRP94 (Santa Cruz Biotechnology, sc1794), Calreticulin (EMD Millipore, 208910), UAP56 (Abcam, ab47955), TIF-1β (Santa Cruz Biotechnology, sc-33186), Fibrillarin (Santa Cruz Biotechnology, sc-25397), GFP (Abcam, ab290), HAT1 (Santa Cruz Biotechnology, sc-8752),cyclin G (Santa Cruz Biotechnology, sc-320), Histone H3 (sc-10809), Coilin (Santa Cruz Biotechnology, sc-32860), TIA-1 (Santa Cruz Biotechnology, sc-1751), LC3 (MBL International), Dcp1α (Abcam, ab47811), HDAC2 (Santa Cruz Biotechnology, sc-7899), G3BP1 (Santa Cruz Biotechnology, sc-98561), PML (Abcam, ab53773), anti-amyloid fibrils OC (EMD Millipore, AB2286), GAPDH (Santa Cruz Biotechnology, sc-25778). Secondary antibodies were HRP- or Alexa-conjugated (Life Technologies). Hoechst (Life Technologies), ethidium bromide (Sigma Aldrich), Congo red (Amresco), Thioflavine S (Sigma Aldrich), Amylo-Glo (Biosensis), NIAD4 (Biovision, 10μM), Methoxy-X04 (Biovision, 20μM), 1-bromo-2,5-bis-(3-hydroxycarbonyl-4-hydroxy) styrylbenzene (Anaspec, 200μM) and hematoxylin/eosin (Sigma) dyes were used.

Stable cell lines, siRNA and transfections. MCF-7 and PC-3 cells stably expressing control and rIGS$_{28}$RNA/rIGS$_{22}$RNA specific shRNA were previously described (Audas et al., 2012). Transfections were performed using Effectene (Qiagen), according to manufacturer's protocol. The following siRNAs were purchased from Ambion: NEAT1 (n509900), MALAT1 (n511399), HOTAIR (n272230), Negative control #1 (4390844), GAPDH positive control (4390849) and custom sequences for rIGS$_{22}$RNA (AGGCACTGTATTGCTACTGGGCT) and rIGS$_{28}$RNA (AATCTAGACAGGCGGGCCTTGCT). PC3 cells were reverse-transfected using RNAiMAX (Life Technologies) and treated/harvested 48 hours post-transfection.

Plasmids. pFLAG-VHL-GFP, pFLAG-POLD1-GFP, pYFP-Tia1, pEGFP-B23, pEGFP-Fibrillarin, pFLAG-RNF8-GFP, pcDNA3.1, pcGFP were previously generated (Audas et al., 2012). Full length cDNA was subcloned into pEGFP-C2 from the Addgene plasmids pcDNA3.1-SC35-cMyc (K. Scotto: Addgene plasmid 44721) and pSCT-GAL93-NONO (S. Brown: Addgene plasmid 46325), while amino acids 1-770 and 18-713 of APP were subcloned into the same plasmid from pCAX-FLAG-APP (D. Selkoe: Addgene plasmid 30154). The following plasmids were purchased from Addgene and used without modification: pEGFP.N1-HDAC6 (T. Yao: Addgene plasmid 36188), pEGFP-coilin (G. Matera: Addgene plasmid 36906) and HSF1-GFPN3 (S. Calderwood: Addgene plasmid 32538). The cDNA encoding UAP56, HDAC2, Ku70, cdk1, Ran, cdk4, HAT1, β-amyloid (amino acids: 1-42), β-amyloid (amino acids: 1-17), P3 (amino acids: 18-42) and fragments of VHL (amino acids: 1-213, 1-36, 34-70, 69-105, 104-140, 122-140, 139-175 and 174-213), cdk1 (amino acids: 100-119, 100-130), HDAC2 (amino acids: 1-33 and 18-60), HAT1 (amino acids: 228-260 and 366-400) and APP (amino acids: 167-209, 209-251, 543-585, 586-628, 629-671 and 723-770) was reverse transcribed from MCF-

7 RNA and inserted into the pET30-LIC (EMD Millipore) and pcTOPO (Life Technologies) cloning vectors with carboxy-terminal GFP tags. Artifical Amyloid Converting Motifs (aACM) derived from POLD1 and VHL were created from linker sequences and sub-cloned into the pET30 and pcTOPO GFP plasmids.

Photobleaching. Fluorescence loss in photobleaching (FLIP) and fluorescence recovery after photobleaching (FRAP) was performed as previously described (Audas et al., 2012) on a Zeiss LSM5 Pascal confocal microscope.

Bacterial inclusion body purification and x-ray diffraction. Bacterial inclusion body purification was modified from (Rodriguez-Carmona et al., 2010). Briefly, 100ml cultures were grown for 20 hours at 32^{o}C, then pelleted and re-suspended in 4ml bacterial lysis buffer (50mM Tris-HCl + 100mM NaCl + 1mM EDTA + 20mM PMSF + 0.1% Triton X100) and incubated for 1 hour at 37^{o}C with gentle agitation. Samples were sonicated on ice for 20 minutes (1 second on, 1 second off) at 40% power (QSonica Sonicators). NP40 (0.8%) was added to lysates and incubated at 4^{o}C with gentle agitation for 1 hour, prior to a 1 hour DNase I treatment at 37^{o}C. Samples were pelleted at 15,000rpm for 15 minutes, washed twice in lysis buffer and re-suspended in ddH_2O. Samples were checked by x-ray diffraction for amyloid content by pelleting down insoluble fractions and then pipeting 2-4 ul of the resulting slurry on mounted nylon loops (1 mm Cryoloops on Crystal Caps from Hampton Research). The resulting drops were allowed to dry in air for 2-3 days and then exposed on X-rays at room temperature. 10 minute exposures were taken on a Rigaku MicroMax 007HF generator using a MAR345 detector at the Scripps Florida X-ray Crystallography Core Facility. Strong reflections were seen at 4.7 Å and 10 Å, which are characteristic of the cross-beta sheet structure in amyloid fibrils (Makin et al., 2006).

Transmission electron microscopy. 2% glutaraldehyde fixed cells were washed and post-fixed in 1% osmium tetroxide. Samples were dehydrated in a series of ascending alcohols and embedded in Epon/Araldite and stained with uranyl acetate and lead citrate. Imaging occurred on a JEOL 1400 transmission electron microscope (Jeol, MA).

Immunofluorescence. Cells were seeded in 3.5 cm plates with 20-mm glass coverslips. Post-treatment, cells were fixed in 4% formaldehyde for 20 minutes and permeablized in 0.5% TritonX-100 for 5 minutes. Cells were incubated for 1 hour with the primary antibody (1:100), washed and incubated for another hour with the secondary antibody (1:300). Hoechst or ethidium bromide was added in PBS for 5 minutes. Congo red and Thioflavine S staining followed established protocols (Guntern et al., 1992; Puchtler and Sweat, 1965; Puchtler et al., 1962). All amyloidophilic dyes were stained used with formaldehyde-fixed cells to minimize background fluorescence. Cells were immersed in 0.05% Congo red or 0.002% Thioflavine S solution for 15 minutes and then washed 3 times in ddH_20. Amylo-Glo staining was modified from Schmued et al. 2012 (Schmued et al., 2012). Fixed cells were rinsed in ddH_20, immersed in 1X Amylo-Glo staining solution for 10 minutes, washed in 0.9% saline for 5 minutes and briefly rinsed in ddH_2O. Slips were mounted and analyzed using an Axio Observer D1 inverted microscope. Images were captured in black and white using an AxioCam MRm and ZEN Pro 2012 software (Carl Zeiss). Artificial color was added using Photoshop CS6 (Adobe). Merged images were generated using ImageJ software. Artificially colored images were combined by Zprojection, with a max intensity projection type.

Western blotting. Western blots were performed using standard techniques. Transferred blots were probed with primary and secondary antibodies described above. Bands were detected by enhanced chemi-luminescence (Luminata Forte, Millipore) on x-ray film.

RNA extractions, analysis and immunoprecipitation. Purified human RNA from multiple tissue types was purchased from Clontech. RNA immunoprecipitation was carried out on transfected MCF-7

cells harvested in lysis buffer (100 mM NaCL, 0.5% Igepal, 20 mM Tris [pH7.6], 5 mM MgCl2, and 1 mM Na3VO4) and sonicated prior to incubation with GFP antibody (Abcam, ab290) and ChIP grade Protein A/G magnetic beads (Pierce). Following washes, RNA was extracted from samples and 10% inputs for RT-PCR.RNA extractions, cDNA synthesis and semi-quantitative PCR were previously described (Audas et al., 2012).

Peptide synthesis and fibrillation assay. Peptides were synthesized by GenScript with the sequences: VHL(104-140) - GTGRRIHSYRGHLWLFRDAGTHDGLLVNQTELFVPS, β-amyloid - DAEFRHDSGYEVHHQKLVFFAEDVGSNKGAIIGLMVGGVVIA and ACM^{VHL} – RRIHSYRLLVNQTELFV. Fibrillation was performed over a 1 week period at 37^{o}C by incubating 1mM peptide in 10mM HCl. Fibrils were detected by transmission electron microscopy.

ATP assay. Cellular ATP concentrations were measured using the CellTiter-Glo Luminescent Assay (Promega) on a LUMIstar Galaxy luminometer (BMG Labtechnologies) according to manufacturer's protocol. Experiments were performed in triplicate.

Flow cytometry. Flow cytometry was conducted on normoxic-neutral, hypoxic-neutral and hypoxic-acidotic cells. Acidosis-permissive media was prepared that reached a final pH of 6.5 and 6.0 as indicated. MCF-7 cells stably-expressing scramble or rIGS_{28}RNA-specific shRNA were grown under the described conditions for 24 hours. Nocodazole (250nM) was added to one plate of each cell line under each condition and treatments continued for 24 hours. Flow cytometry was performed on 70% ethanol fixed cells, washed in phosphate-citrate buffer and treated with 50μl RNase A (100μg/ml) and 450μl propidium iodide (50μg/ml) for 15 minutes prior to analysis (Beckman Coulter Cyan ADP 9 Analyzer).

Staining tissue sections and fluorescence in situ hybridization. Cryo-sections of normal human brain and pancreatic tissue were purchased (Amsbio). Human breast and prostate tumor sections were purchased (Biochain) or obtained from excised masses, respectively. Experiments using human tumors were approved by the University of Miami – Miller School of Medicine institutional review board, with informed consent obtained prior to specimen acquisition. Human tumors, excised mouse xenograft masses were fixed in 10% formalin. All tissue was embedded in paraffin and sliced to a thickness of 3 μm. Human prostate tumors were entirely submitted for histologic evaluation. Primary antibodies were used at a concentration of 1:50 and secondary antibodies at 1:150. Congo red and Amylo-Glo staining was performed as above. Hematoxylin/eosin staining was performed on each section. Fluorescence *in situ* hybridization was performed as described, and with probes previously described (Audas et al., 2012; Jacob et al., 2013).

Statistical analysis. Bars represent the mean value from at least (n values indicated in figure legends) three independent replicates. Statistical analyses were performed with the error bars representing the standard error of the mean. Variances were noted to ensure that they were similar between the compared groups. *p values* were based on two-tailed Student's t-test with the significance level indicated in the figure legend.

Supplementary References

Audas, T.E., Jacob, M.D., and Lee, S. (2012). Immobilization of proteins in the nucleolus by ribosomal intergenic spacer noncoding RNA. Mol Cell *45*, 147-157.

Guntern, R., Bouras, C., Hof, P.R., and Vallet, P.G. (1992). An improved thioflavine S method for staining neurofibrillary tangles and senile plaques in Alzheimer's disease. Experientia *48*, 8-10.

Jacob, M.D., Audas, T.E., Uniacke, J., Trinkle-Mulcahy, L., and Lee, S. (2013). Environmental cues induce a long noncoding RNA-dependent remodeling of the nucleolus. Mol Biol Cell *24*, 2943-2953.

Makin, O.S., Sikorski, P., and Serpell, L.C. (2006). Diffraction to study protein and peptide assemblies. Curr Opin Chem Biol *10*, 417-422.

Puchtler, H., and Sweat, F. (1965). Congo red as a stain for fluorescence microscopy of amyloid. The journal of histochemistry and cytochemistry : official journal of the Histochemistry Society *13*, 693-694.

Puchtler, H., Sweat , F., and Levine, M. (1962). On the Binding of Congo Red by Amyloid. The journal of histochemistry and cytochemistry : official journal of the Histochemistry Society *10*, 355-364.

Rodriguez-Carmona, E., Cano-Garrido, O., Seras-Franzoso, J., Villaverde, A., and Garcia-Fruitos, E. (2010). Isolation of cell-free bacterial inclusion bodies. Microb Cell Fact *9*, 71.

Schmued, L., Raymick, J., Tolleson, W., Sarkar, S., Zhang, Y.H., and Bell-Cohn, A. (2012). Introducing Amylo-Glo, a novel fluorescent amyloid specific histochemical tracer especially suited for multiple labeling and large scale quantification studies. Journal of neuroscience methods *209*, 120-126.